Scientific Research and Essays Vol. 6(20), pp. 4378-4388, 19 September, 2011
Available online at http://www.academicjournals.org/SRE
DOI: 10.5897/SRE10.1163
ISSN 1992-2248 ©2011 Academic Journals

Full Length Research Paper

Effect of waxing on the properties of Al-1Mg P/M alloy

Azim Gökçe[1]* and Fehim Findik[1,2]

[1]Department of Metallurgy Education, Technical Education Faculty, Sakarya University, Sakarya, Turkey.
[2]Department of Mechanical Engineering, Faculty of Engineering and Natural Sciences, Sarajevo, Bosnia-Herzegovina.

Accepted 15 August, 2011

In the current work, 1wt% Acrawax was premixed with the aluminium and magnesium powder as a lubricant for the first group samples. However, no wax was used for the second group specimens. As a sintering aid, 1 wt% Mg was added for both group materials. Compaction of the specimens was performed using a manual Carver hydraulic press and a floating rectangular die. First group specimens were pressed to green densities of 91.5 and 92.5% using pressures of 435 and 490 MPa, respectively. In the second group (no wax) samples, 93% green density was obtained using the similar compaction pressures. These conditions produced specimens whose dimensions were: 31.8 × 12.7 × 3.5 mm^3. As a result, an increase has been seen on the density of sintered and green compacts with rising compacting pressure. Furthermore, addition of the wax negatively affected the transverse rupture strength of the alloy.

Key words: Powder metallurgy, aluminum, sintering, microstructure, mechanical properties.

INTRODUCTION

Al and its alloys have good mechanical strength and corrosion resistance, low density and cost advantages depending on the manufacturing method, as well as, higher thermal and electrical conductivities (Hunt, 2000). The announcement and fabrication of light weight and near net shape high quality Al alloys by powder metallurgy (PM) has grown in particular for aerospace and automotive purposes (Beaumont, 2000). Yet, there are a number of complexities in the straight compaction and sintering of almost every series of Al powder. This difficulty is a result of the existence of a firm and intense oxide layer covering the powder particles and therefore dropping both the compressibility and sinterability of the powder. Various attempts have been made effectively to develop the compressibility and the sintering response in different ways and for diverse series of Al alloys. It is confirmed (Lumley et al., 1999; Kondoh et al., 2001) that an addition of 0.1 to 1 wt% Mg facilitates to break up the surface oxide layer through the development of a MgAl2O4 phase (Lumley et al., 1999). This enhanced the sintered density by 9% with 1 wt% Mg content and for this reason enhanced the mechanical features (Kondoh et al., 2001). The new scientists (Martin et al., 2002) have concluded that rising the Mg content equal to 3.5 wt % in 7xxx series enhanced the mechanical strength better than the present commercial alloy. Moreover, it was mentioned (Lumley and Schaffer, 1996) that at elevated Mg contents, the inferior phase could not be completely dissolved in solid solution and therefore stayed as a complex at the grain boundaries resulting embrittlement of the alloy. Conversely, major developments in the sinterability of diverse Al alloys (primarily 7xxx and 2xxx series) have been published (Lumley and Schaffer, 1996; Schaffer et al., 2001). This was feasible by a liquid phase sintering (LPS) course resulting to enhance densification of the alloys. In the reported papers, the cause of trace addition of chosen elements such as Pb, Sn and Sb on the sinterability of Al alloys was examined (Martin et al., 2002; Lumley and Schaffer, 1996; Schaffer et al., 2001; Schaffer and Huo, 1999; Sercombe and Schaffer, 1999; Sercombe, 2003). It was understood that microalloying with 100 ppm of Pb (0.12 wt% Pb) supplied the superlative sintering reaction and enhanced the ultimate tensile strength (UTS) by 36% from 214 to 427 MPa of an Al-Zn-Mg-Cu alloy formed from premixed elemental powders (Sercombe, 2003). It was affirmed that the admixed elements such as Pb and Sn had low solubility

*Corresponding author. E-mail: azimg@sakarya.edu.tr. Tel: +902642956499. Fax: +902642956424.

Table 1. The properties of the used materials and lubricant.

Materials	Company	Properties
Al	Cerac	Composition: 99.5% (purity) Particle size: -100/+200 mesh (-150/+75 µm).
Mg	Cerac	Composition: 99.6% (purity) Particle size: -200/+325 mesh (-75/+45 µm).
Acrawax	Lonza Inc.	Material: Acrawax C lubricant chemical name: ethylene bis-stearamide (EBS). Physical state: powder. Density: 0.97 g/cm^3. Flash point: 285°C. Boiling point: 260°C. Melting point: 140 - 145°C.

in the base Al matrix and consequently stayed segregated at the liquid/vapor interface. A researcher (Martin and Castro, 2003) measured the densification behavior of the 2xxx, 6xxx and 7xxx series Al powder mixtures under various sintering circumstances including temperature, time and atmosphere as well as diverse heat treatment. It was recognized that the 2xxx series compacted at 400 MPa presented a little higher density (95% TD) when sintered under a vacuum as compared with sintering in nitrogen (92% TD). On the other hand, both the 6xxx and 7xxx series Al powder mixtures also pressed at 400 MPa, illustrating much better sinterabilities by sintering in nitrogen and reaching densities of 97% TD.

An accomplishment was obtained (Ziani and Pelletier, 1999a, b) for degassed 6061 Al prealloyed powder by supersolidus liquid phase sintering (SLPS) subsequent to vacuum degassing of the prealloyed powder, compaction at 380 MPa and high compaction pressure of 760 MPa by sintering under argon at 585, 605 and 625°C for 30 min. Green and sintered densities in the range of 2.61 to 2.68 g cm^{-3} and 2.59 to 2.68 g cm^{-3} were gained, respectively, which resulted in tensile strength of 335 MPa with 7% elongation for the fully heat treated (T6) 6061 alloy. It has also been reported (Schaffer et al., 2002) that segregation and delubrication can be an important issue with processing of PM Al alloys if an appropriate lubricant has not been used. This can cause potentially unsafe surroundings with inhomogeneity and delubrication defects within the sintered product. Hence, some of the presented lubricants used for the Fe based PM alloys are not appropriate for the Al based powders due to their burning properties reasoning undesirable reactions by products. It was stated that the compaction, sintering and mechanical properties of the premixed elemental 6061 Al powder was with and without addition of sintering aids (Pb, Sn or Ag) (Showaiter et al., 2005). In this paper it was obtained that by normal compaction at 340 or 510 MPa and sintering under pure nitrogen (30 min or 1 h), sintered densities of ≥2.68 g cm^{-3} (98% TD) were accessible. Also this process resulted in UTS of 305 MPa and 6 to 8% elongation for the (sintered and) fully heat treated (T6) 6061 Al alloy. The premixed elemental powder caused the development of two types of liquid phase during sintering. Lately, two papers (Youseffi et al., 2006; Youseffi and Showaiter, 2006) have been published about physical and mechanical properties of the received (gas atomized) and degassed 6061 Al prealloyed powders with and without additions of solid or liquid lubricants and sintering aids (Pb, Sn or Ag). Both vacuum and pure nitrogen sintering were carried out for compaction at 340 or 510 MPa and also to investigate the effect of sintering atmosphere for the prealloyed 6061 Al powder compacts. Highest sintering densities of ~98 to 99% of theoretical were obtained for the prealloyed (and degassed) Al compacts by sintering under pure nitrogen with an addition of paraffin wax, liquid paraffin or a Pb addition as a sintering aid and no lubricant. It was found that additions of solid lubricants such as lithium stearate and acrawax to both the premixed and prealloyed powders reasonable green densities, but had deleterious effect on sintered densities and microstructures. Other lubricants such as zinc stearate, stearic acid and liquid paraffin provided similar green densities, but higher sintered densities and less porous microstructures.

In the present study, the physical and mechanical properties are compared for argon atomized Al-1 wt-% Mg powders with and without lubricant 1 wt % Acrawax. Pure nitrogen sintering was performed and the effect of sintering atmosphere for the mixed Al-1% Mg powder compacts was investigated.

MATERIALS AND METHODS

Mixing

Argon atomized Al and 1% Mg and also adding 1 Acrawax (all w/o) in the second group samples are mixed and shaked for 20 min. The properties of the used materials and lubricant are shown in Table 1. The shape and morphology of the metal powders were also

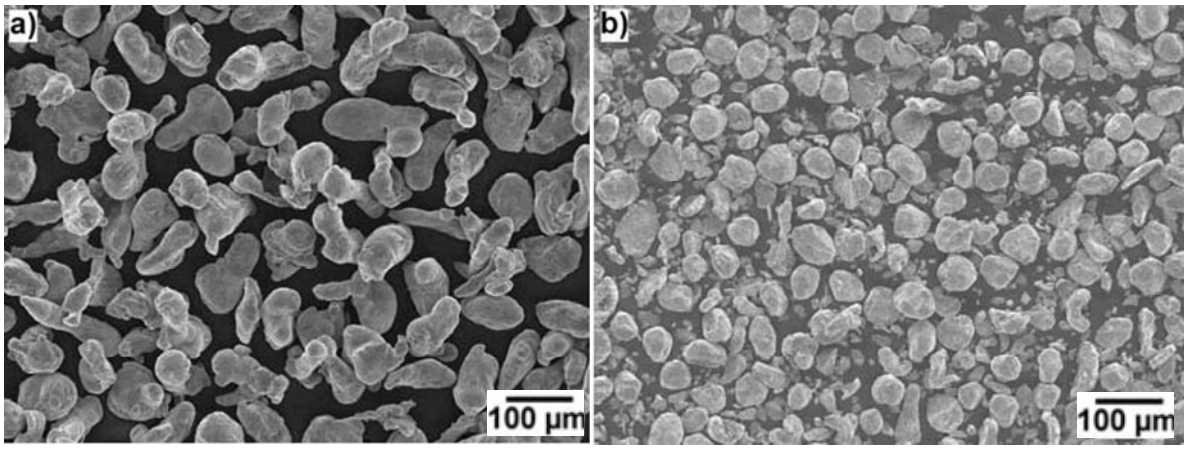

Figure 1. Representative particle morphology of argon atomized. a) Al powder, and b) Mg powder; sieved below 150 µm showing rounded but irregular Al particles and sieved below 75 µm showing mostly spherical Mg particles.

inspected using SEM and representative particle morphologies as shown in Figure 1.

Compaction and sintering

For each compaction, ~3.5 g of powder was used and poured into the die cavity. Care was taken to make sure that the powder was dispersed properly within the die cavity. Rectangular specimens with the size of 31.8 × 12.7 × 3.5 mm (3.5 g of powder) were pressed at pressures in the range of 330 to 490 MPa for the mixed powders in order to study the compaction properties and consequently to observe the best compaction pressure for sintering. Also, these rectangular bars were used for mechanical testing. A single performing hydraulic press (22 ton Carver) was employed for compaction. Sintering was carried out under pure nitrogen atmosphere (about -50°C dew point) in a standard carbolite gas atmosphere, recrystallized alumina tube furnace (controlled by a Eurotherm 2404 controller) at a temperature of 640°C for 2 or 6 h. The green and sintering densities were calculated by measuring the dimensions and weight of the specimens to an accuracy of 0.001 mm and 0.0001 g respectively.

Metallography and mechanical testing

Same sized specimens were used for the three point bending machine. To do this an INSTRON 5869 machine having the 1000 kN maximum load was employed using 25.4 mm span between the lower supports and 2 mm/min strain rate. Microstructural examination of the Al-1 Mg alloy was conducted using a JEOL JSM-6500F scanning electron microscope (SEM). The quantitative analysis of the microstructure within the sintered specimens was performed using the SEM equipped with an energy disperive spectroscopy (EDS). Metallographic samples were prepared conventionally, and then polished using 6 mm and finished with 1 mm polish. No etching was carried out.

RESULTS

Compaction behavior

The mixed Al-1% Mg powders with and without wax were compacted at different pressures in the range of 330 to 490 Mpa to study their compressibility. The admixed lubricant has improved the green density from ~2.41 g cm^{-3} (without lubricant mixed powder) to ~2.45 to 2.48 g cm^{-3} as expected. The mixed powders with 1% Acrawax (w/o) were pressed at 435 and 490 MPa, and sintered at 640°C for 2 h under pure nitrogen atmosphere. The same conditions were used for the no wax samples; however the sintering time was extended to 6 h instead of 2. Figure 2 shows the compaction graph by plotting green density versus compaction pressure. It is seen from Figure 2 that green and theoretical density increased with the increment of compaction pressure. This is consistent with the previous work (Youseffi et al., 2006; Youseffi and Showaiter, 2006; Simchi and Vltl, 2003). In the present study, the theoretical density (density of loose Al-Mg-Acrawax powder) was found as 2.6852 (±0.0043) g/cm^3. According to this value, the average calculated green density of the wax included samples is obtained as 2.4564 g/cm^3 using 435 MPa compression pressure, it means that the material is 91.5% dense (8.5% porosity) in the present work. When higher compression pressure, 495 MPa has been applied to the powders, the average calculated green density of the samples is obtained as 2.4840 g/cm^3, it means produced samples have 7.5% porosity. The theoretical density (density of loose Al-Mg-no wax) was found as 2.7125 (±0.0030) g/cm^3. After compression with a pressure of 435 MPa 2.5186 g/cm^3 (92.8% dense) green density has been achieved. When compression pressure was increased from 435 to 490 MPa green density of the samples decreased to 2.5103 g/cm^3 (92.5% dense).

Sintering effect

Al-1 Mg powders with wax specimens were sintered in two steps within the nitrogen atmosphere: first, specimens

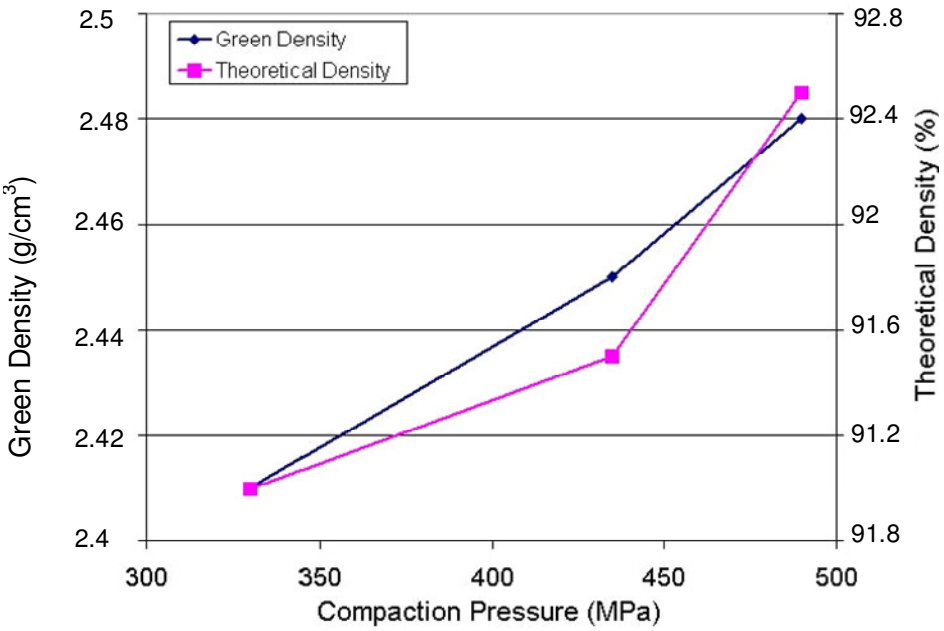

Figure 2. The relationship between compaction pressure and green/theoretical density for various Al-1% Mg compacted samples.

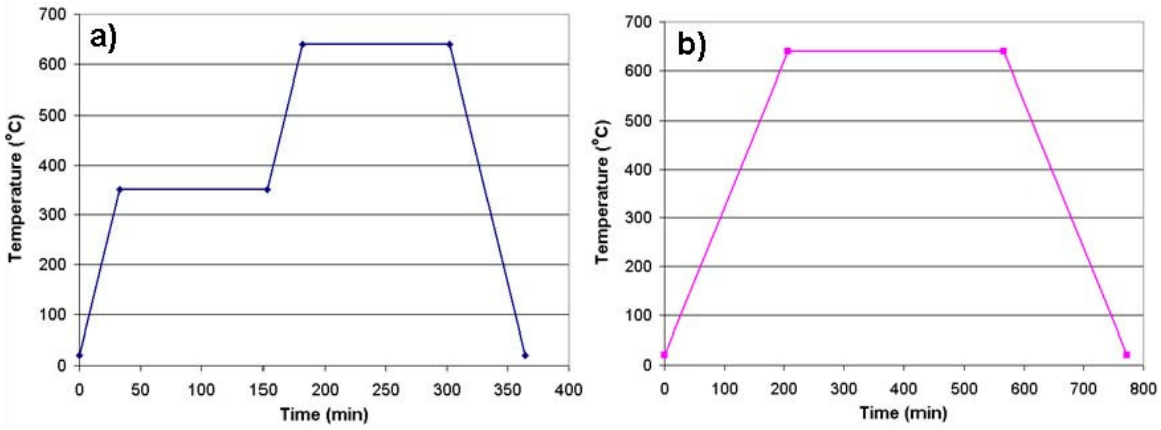

Figure 3. Sintering time versus temperature for a) Al-1% Mg-1%Acrawax compacts and b) Al-1 Mg (all w/o).

were heated to 350°C for 2 h for polymer burn out and then the temperature was ramped up to 640°C for 2 h and finally the furnace cooled down to room temperature. The heating and cooling speed was 10°C/min and the dew point of N2 was about -40°C. The Eurotherm 2404 temperature controller was used in the muffle furnace. Figure 3a depicts the temperature and sintering time relationship for the present study. Al-1 Mg compacts (no wax) were sintered in the same furnace at the same atmosphere (N2), but in a one step process. Specimens were heated at the same temperature (640°C), but for longer (6 h) than the others and finally furnace cooled down to room temperature (Figure 3b). The heating and cooling speed was slower than before (3°C/min). In wax added specimens applying 435 MPa commpression pressure, average sintering density is equal to 2.2698 g/cm^{-3} which is 84.5% density (15.5% porosity). It means that porosity is doubled during the sintering process compared to the green one. The large porosities reduced the sintering densities due to a wide polymer burn off range leaving residual porosity. In addition, sintering density decreased in 10%. In case of using 490 MPa pressure (Table 2), the obtained average sintering density is identical to 2.2707 g/cm^{-3} which is 84.5% density

Table 2. Green and sintered densities of Al-1 Mg (with and without wax) pressed at 435 and 490 MPa.

Powder type	Compacting pressure (MPa)	Theoretical density (g/cm^{-3})	Green density (g/cm^{-3})	%TD	Sintered density (g/cm^{-3})	%TD
Al-1 Mg-1 wax	435	2.6852	2.4564	91.5	2.2698	84.5
Al-1 Mg		2.7125	2.5186	92.8	2.5988	95.8
Al-1 Mg-1 wax	490	2.6852	2.4840	92.5	2.2707	84.5
Al-1 Mg		2.7125	2.5103	92.5	2.5791	95.1

(15.5% porosity). It represents that porosity is twofolded during the sintering route compared to the green one. This is due to formation of large porosities during the sintering stage for the polymer burn out and as a result material is expanded, volume increased and density decreased. Comparing Al-1 Mg powders with and without wax, unwaxed samples gave better green and sintered density for both pressures (Table 2). Although Acrawax lubricant provides a reasonable green density, it had a deleterious effect on sintered density mainly owing to its wide burn off range and hence incomplete removal during sintering leaving some black residue. The previous workers (Youseffi et al., 2006) reported that the best green and sintered densities were obtained with paraffin wax and liquid paraffin which had a shorter burn off range leaving no residue after sintering and hence a cleaner end product. They concluded that the higher the molecular weight, the wider the burn off range and the more reactive with Al the less suitable the lubricant.

The present results are consistent with the previous works (Youseffi et al., 2006; Youseffi and Showaiter, 2006; Simchi and Vltl, 2003). In the current study, density decreased due to wax burn out as explained earlier, it increased owing to the AlN formation. Because, sintering under nitrogen was beneficial for its reducing atmosphere, protection against further oxidation, reducing the oxide content of the Al powder particles and formation of AlN (Mondolofo, 1976) which improves the densification as ~2.60 g cm^{-3} (~95.8% TD) pressed at 435 MPa.

DISCUSSION

In this particular section, first microstructural evaluation will be discussed under the three subsections and then alteration of mechanical properties will also be argued.

Microstructural evaluation

Specimens of the as sintered in pure nitrogen mixed Al-1 Mg samples with lubricant, pressed at 435 or 490 MPa and sintered at 640°C for 2 h were prepared conventionally for metallographic examination using a scanning electron microscope. Porosity content, pore size, shape and distribution within the sintered samples were inspected using an SEM equipped with EDS analysis. Residual macro- and microporosity was present in all sintered samples under every sintering condition. Medium sized pores and small interconnected micro-pores at grain boundaries were visible when lubricant was added which reduced the sintered densities due to a wide burn off range leaving residual porosity.

Fracture surfaces

After the three point bending test, the fracture surfaces were examined in the SEM using different magnifications. It is observed that sintering is quite successful in the outer side of the specimens; it is not properly sintered in the inner side of the specimens for both group specimens. The reason could be due to insufficient sintering time or the rapid heating rate of 10°C/min. Most likely, diffusion is not sufficiently completed within such a ramp rate condition at 640°C for 2 h. The representative SEM micrographs are shown in Figure 4 samples of Al-1 Mg-1 Wax sintered compacts. In Figure 5, fracture surfaces are seen for a sintered Al-1 Mg powder (sintered at 640°C for 6 h) with a density of 84.5%. Brittle fracture occurred at the interparticle necks, indicating that strength is controlled by interparticle bonds. It is also seen that the interparticle necks are not formed in everywhere; it implies that sintering is not properly achieved. It needs extra time or slower process to accomplish the sintering technique. This problem is due to the oxidation of aluminum, since aluminum is always covered by an oxide film. The

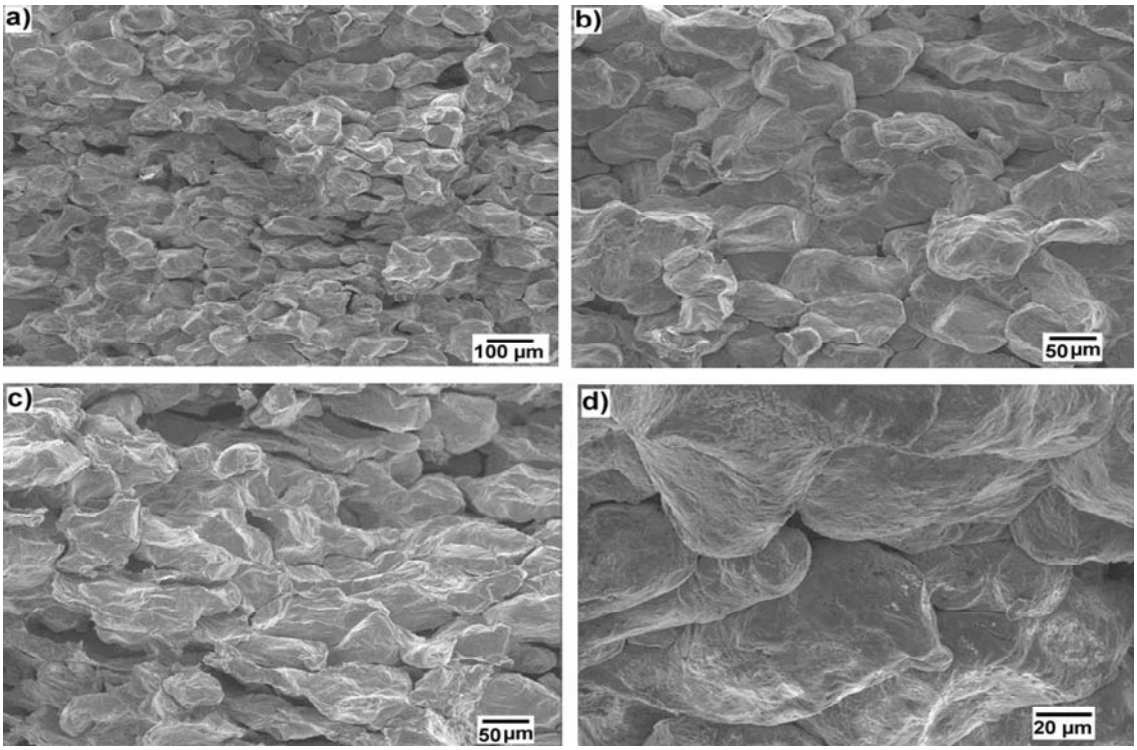

Figure 4. SEM micrographs of Al-1 Mg-1 wax specimens for fracture surfaces after three point bending test. Some porosities and cracks are seen. Sufficient sintering in outer sides and less in the inner side. Figures 4a and 4b belong to 435 MPa, 4c and 4d 490 MPa compression pressures.

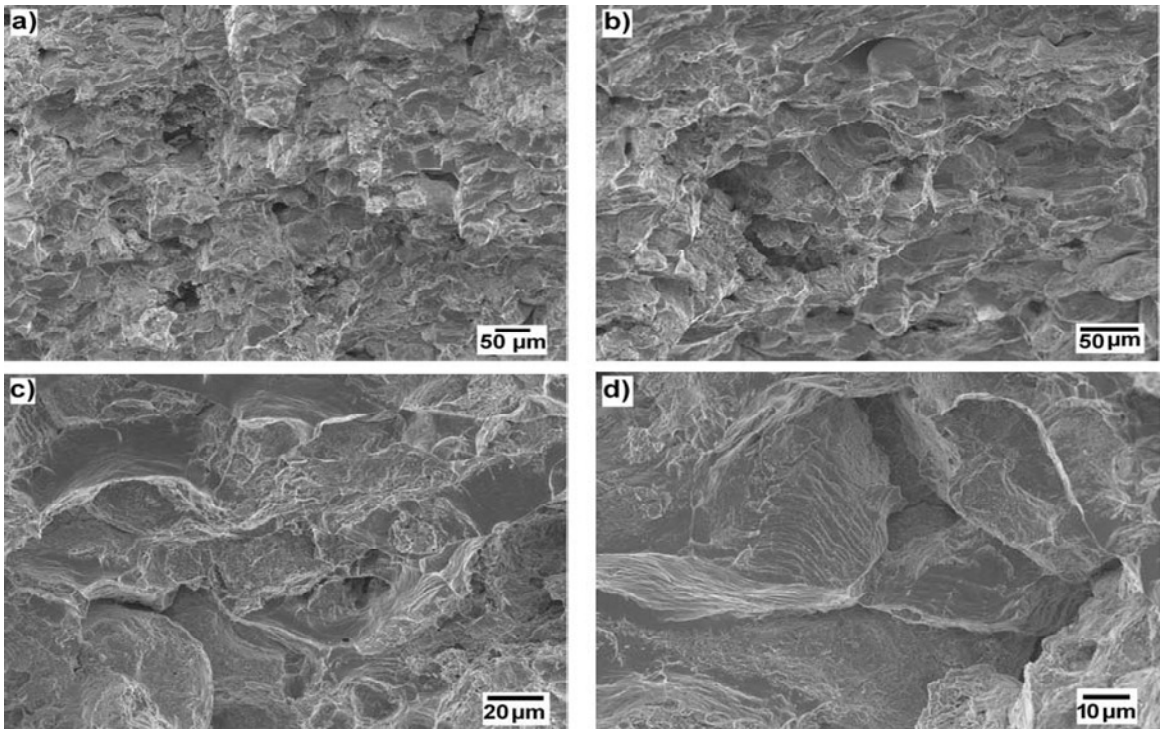

Figure 5. SEM micrographs of Al-1 Mg specimens for fracture surfaces after three point bending test. Some porosities and cracks are seen. Evidences of sufficient sintering is visible in everywhere. Figures 5a and 5b belong to 435 MPa, Figures 5c and 5d 490 MPa compression pressures.

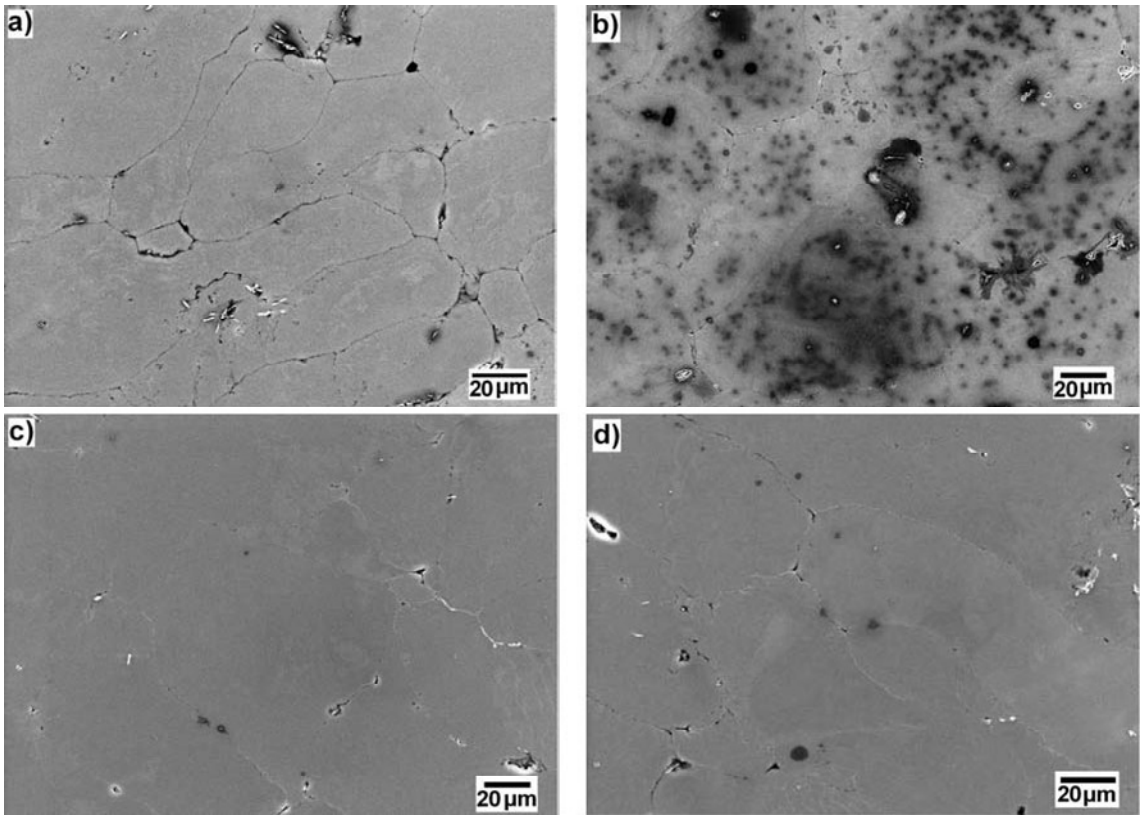

Figure 6. SEM micrographs of cross-section view for sintered Al-1 Mg-1 wax sintered and polished samples. Some irregular porosities mainly in grain boundaries and also surface porosities are clearly seen as black spots in upper right micrograph. Figures 6a and 6b belong to 435 MPa, 6c and 6d 490 MPa compression pressures.

thickness of the oxide is dependant on the temperature at which it formed and the atmosphere in which it is stored, particularly the humidity. Fresh oxide on bulk aluminum at room temperature is widely reported as being 10 to 20 Å thick. The thickness on atomized powder can vary from 50 to 150 Å. The oxide on aluminum is usually amorphous and hydrated with an adsorbed water layer. The oxide crystallizes to γ-Al_2O_3 on prolonged annealing at temperatures above 350°C (Bishop et al., 2000). The oxide prevents solid state sintering in low melting point metals, including aluminum. This has been explained in terms of the relative diffusion rates through the oxide and the metal, for metals with stable oxides (Bishop et al., 2000).

The use of liquid phases is an alternative to solid state sintering. However, ductile fracture is clearly visible in Figure 5 for both pressured samples due to perfect diffusion at slower heating rate (3°C/min) and also longer sintering time (6 h) at the same sintering temperature (640°C) in nitrogen atmosphere. In general, there are a large number of dimples, which were elongated parallel to the fracture surface. These observations indicate that the cracks mainly grew through a transgranular mode and that shear stress affected crack growth during bending deformation.

Cross-section view

In order to understand the sintering effect and see the porosities, the specimens are cut verticularly, polished and the cross-section area is examined in SEM (Figures 6 to 7). It is seen from Figures 6 and 7 that some irregular porosities mainly in grain boundaries and also surface porosities are clearly seen as black spots in several micrographs. However, more porosities in wax added samples were compared to unwaxed ones due to wide polymer burn off process during the sintering time. It is seen from the sintered polished samples, cross-section view (Figure 6 to 7) and fracture surfaces (Figure 5) that solid state sintering occurred in Al-Mg system. Due to surface and grain boundary diffusion, necks formed between the sintered particles at sufficient temperature (630°C) and time (90 mins). This is consistent with the previous literature (Ziani and Pelletier, 1999a, b).

EDS analysis

The elemental microanalysis of various grain boundaries and also matrix were conducted using EDS analysis (Table 3 and Figure 8). The present structure contains

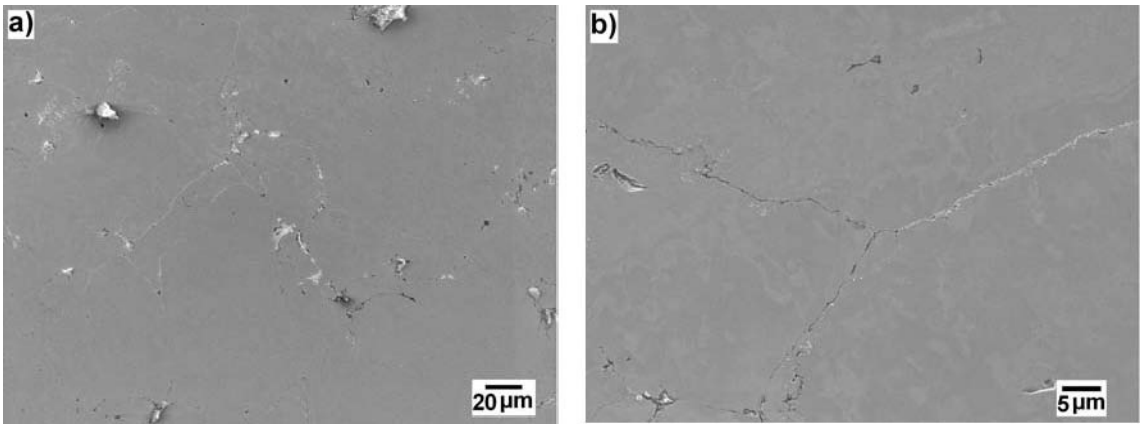

Figure 7. SEM micrographs of cross-section view for sintered Al-1 Mg sintered and polished samples. Some irregular porosities mainly in grain boundaries and also surface porosities are clearly seen as black spots in upper right micrograph. Both of the micrographs belong to 435 MPa compression pressures.

Table 3. EDS analysis of points showed on Figure 8.

Spectrum	Elements (% wt)							
	C	N	O	Mg	Al	Si	Fe	Ni
Spectrum 1	1.78	3.13	37.04	34.39	22.88	0.78	-	-
Spectrum 4	0.83	1.89	16.04	3.25	63.28	5.60	8.49	0.61

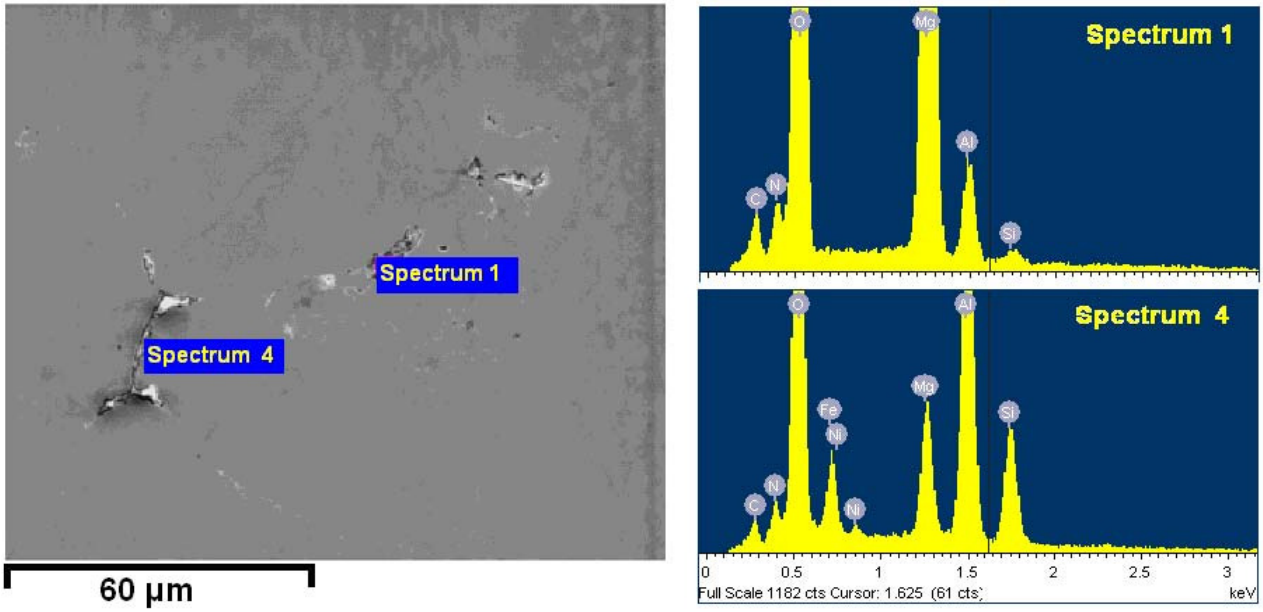

Figure 8. SEM micragh and EDS analysis in Al-1 Mg compaction under 435 MPa, Spectrum 1 illustrating Mg_2Si phase in grain boundary and Spectrum 4 illustrating Al-Fe-Si phase in grain boundary.

basicaly Al and Mg. However, it can also be observed that some impurities such as Si are present in the structure (Table 3). In addition, O can also be observed due to high affinity of Al and Mg in the ambient temperature (Figure 8). The presence of grain boundary solidified liquid phases, analysed by EDS system was

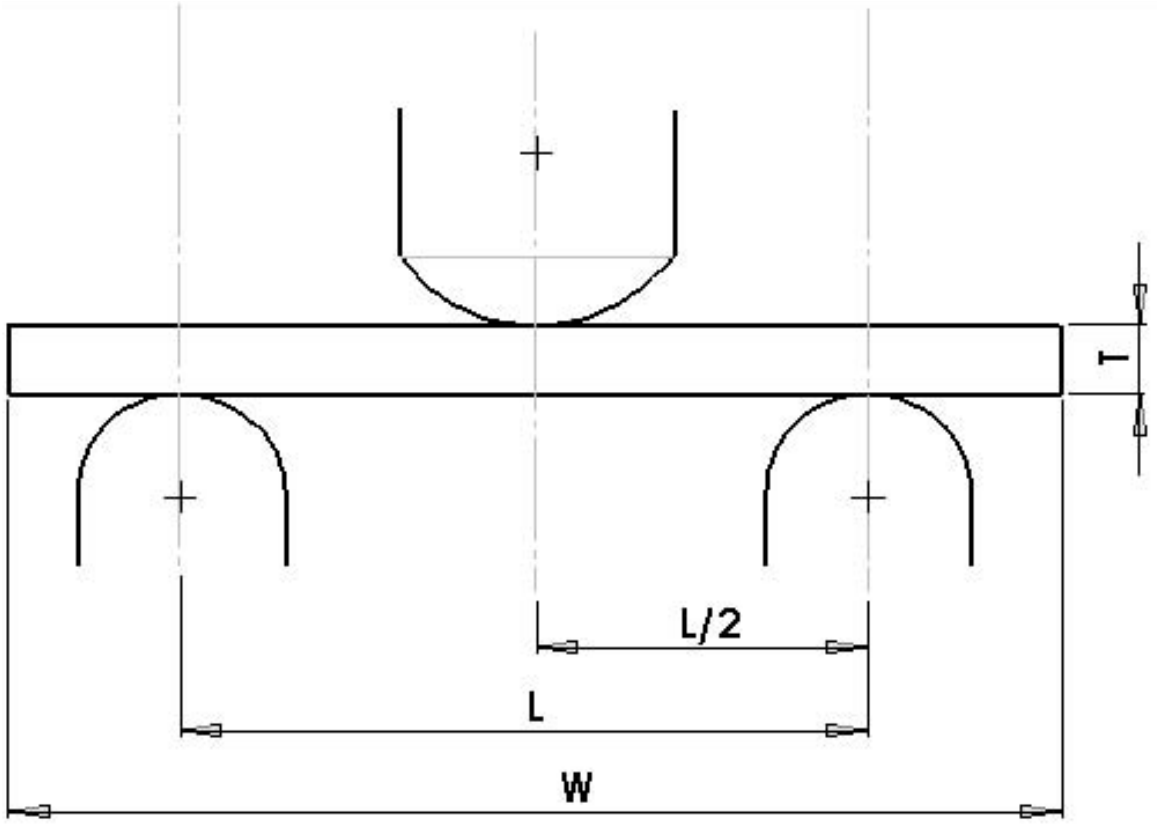

Figure 9. Schematic view of three point bending test.

almost consistent in all the sintered compacts, that is light grey structures of Al-Fe-Si phase (Figure 9) are exposed at grain boundaries with iron being one of the main impurities of the received Al powders. A dark grey phase, mostly at grain boundaries was analysed as mainly Mg_2Si (Figure 9) which forms due to rapid solidification of the gas/air atomized Al powder reasoning supersaturation of Mg/Si in the solid solution and precipitating in the form of fine Mg_2Si upon exposure to high temperatures during sintering (Youseffi and Showaiter, 2006). Presence of this phase has also been confirmed from the Al-Mg-Si phase diagram by other researchers (Philips, 1959). Some fine black areas that appeared in both group samples also appeared in both alloys as remaining fragments of the aluminum oxide of the starting Al powder.

Mechanical properties alteration

Three point bending test was employed to check the mechanical properties of sintered Al-1 Mg compacts using the INSTRON 5869 machine having the 1000 kN maximum load. In the present test, 2 mm/min strain rate was used and the distance (span) between the lower support rods was 25.4 mm which was suggested by the related standard (ASTM D 790-92). The 3 specimens from each group were examined and the average results were reported. In Figure 9, schematic view of three point bending test is illustrated. Transverse rupture strength (TRS) was calculated using the equation (German, 2005; MPIF, 2006) as follows:

$$\sigma T = 3FBL/2WT^2 \quad (1)$$

Here, σT is transfer rupture strength, FB is failure load, L is distance between the lower support rods, W is the width of the specimen and T is the thickness of the specimen. The calculated results for with and without waxed powders are shown in Tables 4 and 5 for 435 and 490 MPa compression pressure, respectively. Span length was 25.4 mm for all of the specimens.

It is seen from Table 4 that TRS is found as between 20.2 to 26.1 Mpa for the three Al specimens and the average TRS is calculated as 22.5 (±1.97) MPa. It is also noticed from Table 4 that TRS is found between 194 to 25.0 Mpa for the three Al specimens and the average TRS is calculated as 22.0 (±1.87) MPa. It shows that their mechanical performance is weak during the transverse rupture (three point bending test) due to insufficient sintering conditions. It is seen from Table 5 that TRS is found between 200 to 218 Mpa for the three Al specimens

Table 4. The mechanical properties of Al-1%, Mg-1% Acrawax (all w/o) applied 435 and 490 MPa compression pressure and sintered at 640°C 2 h exposed to three point bending test.

Specimen no	Compression pressure (MPa)	Failure load (N)	W (mm)	T (mm)	TRS (MPa)
4		80	12.93	3.42	20.2
5	435	100	12.93	3.36	26.1
6		80	12.91	3.34	21.2
4		125	12.99	3.83	25.0
5	490	110	13.00	3.86	21.6
6		100	13.00	3.89	19.4

Table 5. The properties of Al-1 Mg (w/o) compacted under 435 and 490 MPa compression pressure exposed to three point bending test.

Specimen no	Compression pressure (MPa)	Failure load (N)	W (mm)	T (mm)	TRS (MPa)
2		550	12.73	2.86	200.93
3	435	500	12.77	2.73	200.16
4		550	12.70	2.75	218.18
1		660	12.80	2.84	243.57
2	490	630	12.70	2.95	217.18
3		580	12.74	2.90	206.24

and the average TRS is calculated as 206.42 (±6.01) MPa. It is also observed from Table 5 that TRS is found as between 206 to 243 Mpa for the three Al specimens and the average TRS is calculated as 222.33 (±12.44) MPa. It shows that their mechanical performance is very good for both pressures during the transverse rupture (three point bending test) owing to enhanced diffusion in the mentioned sintering process. Mechanical properties of the studied Al alloys were significantly better than those obtained for the equivalent alloys produced via premixed elemental powders, sintered under pure nitrogen as reported previously (Showaiter et al., 2005). However, from the sintered and tempered microstructures, it became clear that the grain boundary microporosity could not be eliminated completely even by sintering under vacuum or pure nitrogen and slow cooling rate. This meant that the remaining discontinuous oxide layers reduced sinterability causing rather poor bonding at prior grain boundaries. It follows, therefore that the highest TRS properties (of ~400 MPa for TRS) for this Al grade can only be obtained via degassing and hot extrusion (and T6 temper) so as to cause a more homogeneous oxide distribution as well as strengthening through oxide dispersion (Alcald Aluminum, 2008).

Conclusion

The following are the conclusions:

a) Green and theoretical density increased with the increment of compaction pressure. In the present study, green density for wax added samples were found as 91.5 and 92.5% for 435 and 490 MPa compression pressure, respectively. However, no wax samples gave a green density of 92.8 and 92.5% for the same pressures.
b) Although Acrawax lubricant provides a reasonable green density, it had a deleterios effect on sintered density mainly owing to its wide burn off range and hence incomplete removal during sintering leaving some black residue.
c) In grain boundary analysis, the light grey structures of Al-Fe-Si phase and a dark grey phase, mostly at grain boundaries was analyzed as Mg_2Si which forms due to rapid solidification of the gas/air atomized Al powder reasoning supersaturation of Mg/Si in the solid solution and precipitating in the form of fine Mg_2Si upon exposure to high temperatures during sintering.
d) Residual macro- and microporosity was present in all sintered samples under every sintering condition.

Medium sized pores and small interconnected micro-pores at grain boundaries were visible when lubricant was added which reduced the sintered densities due to a wide burn off range leaving residual porosity.
e) It shows that the mechanical performance of the sintered samples with lubricant was weak (~20 MPa) during the transverse rupture stress (TRS or three point bending test). Conversely, TRS improved 20 times (>200 MPa) in wax free samples.

ACKNOWLEDGEMENTS

One of the authors (FF) wishes to thank the rectorate of Sakarya University (Sakarya, Turkey) and Center for Advanced Vehicular Systems in Mississippi State University for financial support of the research program.

REFERENCES

Beaumont FV (2000). Aluminum P/M: past, Present and Future. Int. J. Powder Metall., 36(6): 41-44.
Bishop DP, Cahoon JR, Chaturvedi MC, Kipouros GJ, Caley WF (2000). Mat Sci Eng A-Struct., 290(1-2): 16-24.
German RM (2005). Powder Metallurgy and Particulate Materials Processing. MPIF. Princeton.
Hunt WH (2000). New directions in aluminum-based P/M materials for automotive applications. Int. J. Powder Metall. 36(6): 51-60.
Kondoh K, Kimura A, Watanabe R (2001). Effect of Mg on sintering phenomenon of aluminium alloy powder particle. Powder Metall, 44(2): 161-164.
Lumley R, Sercombe T, Schaffer G (1999). Surface oxide and the role of magnesium during the sintering of aluminum. Metall Mater. Trans. A., 30(2): 457-463.
Lumley RN, Schaffer GB (1996). The effect of solubility and particle size on liquid phase sintering. Scripta Mater., 35(5): 589-595.
Martin JM, Castro F (2003). Liquid phase sintering of P/M aluminium alloys: Effect of processing conditions. J. Mater. Process Tech., (143): 814-821.
Martin JM, Gomez-Acebo T, Castro F (2002). Sintering behaviour and mechanical properties of PM Al-Zn-Mg-Cu alloy containing elemental Mg additions. Powder Metall., 45(2): 173-180.
Mondolofo LF (1976). Aluminum alloys: structure and propertries. Butterworths. London.
MPIF Standard (2006). Method for Determination of Transverse Rupture Strength of Powder Metallurgy Materials. MPIF Standard Test Methods.
Phillips HWL (1959). Annotated equilibrium diagrams of some aluminum alloy systems. The Institute of Metals. London.
Schaffer GB, Huo SH, Lumley RN (2002). Binder treatment and lubricant system for aluminium P/M. Int. J. Powder Metall., 38(8): 35-43.
Schaffer GB, Huo SH (1999). On development of sintered 7*xxx* series aluminium alloys. Powder Metall., 42(3): 219-226.
Schaffer GB, Sercombe TB, Lumley RN (2001). Liquid phase sintering of aluminium alloys. Mater. Chem. Phys., 67(1-3): 85-91.
Sercombe TB (2003). On the sintering of uncompacted, pre-alloyed Al powder alloys. Mat Sci Eng A-Struct., 34(1-2): 163-168.
Sercombe TB, Schaffer GB (1999). The effect of trace elements on the sintering of Al-Cu alloys. Acta Mater., 47(2): 689-697.
Showaiter N, Youseffi M, Martyn MT (2005). Part I- Elemental 6061 Al alloy powder with and without Pb, Sn or Ag addition as sintering aids. In 2nd Int. Conf. on 'Advances in Production and Processing of Aluminum: Proceedings of an international conference held at Bahrain, Kingdom of Bahrain. pp. 1-19.
Simchi A, Vltl G (2003). Investigation of warm compaction and sintering behaviour of aluminium alloys. Powder Metall, 46(2): 159-164.
The Online Materials Database. Alcald Aluminum 6061.T6. T651
URL address: http://www.matweb.com/search/DataSheet.aspx?MatID=9391&ckck=1, Last Login: 04.03.2008 12:16 pm.
Youseffi M, Showaiter N (2006). PM processing of elemental and prealloyed 6061 aluminium alloy with and without common lubricants and sintering aids. Powder Metall, 49(3): 240-252.
Youseffi M, Showaiter N, Martyn MT (2006). Sintering and mechanical properties of prealloyed 6061 Al powder with and without common lubricants and sintering aids. Powder Metall., 49(1): 86-95.
Ziani A, Pelletier S (1999). Sintered 6061 Al prealloyed powder: processing and mechanical behavior. Int. J. Powder Metall., 35(8): 49-59.
Ziani A, Pelletier S (1999). Supersolidus liquid-phase sintering behavior of degased 6061 Al powder. Int. J. Powder Metall., 35(8): 59-65.